npg

ARTICLE

Generation of X-CGD cells for vector evaluation from healthy donor CD34+ HSCs by shRNA-mediated knock down of gp91phox

Christian Brendel[1,2], Kerstin B Kaufmann[1], Anja Krattenmacher[1,3], Shweta Pahujani[1] and Manuel Grez[1]

Innovative approaches for the treatment of rare inherited diseases are hampered by limited availability of patient derived samples for preclinical research. This also applies for the evaluation of novel vector systems for the gene therapy of monogenic hemato-logical diseases like X-linked chronic granulomatous disease (X-CGD), a severe primary immunodeficiency caused by mutations in the gp91phox subunit of the phagocytic NADPH oxidase. Since current gene therapy protocols involve *ex vivo* gene modification of autologous CD34+ hematopoietic stem cells (HSC), the ideal preclinical model should simulate faithfully this procedure. However, the low availability of patient-derived CD34+ cells limits the feasibility of this approach. Here, we describe a straightforward experimental strategy that circumvents this limitation. The knock down of gp91phox expression upon lentiviral delivery of shRNAs into CD34+ cells from healthy donors generates sufficient amounts of X-CGD CD34+ cells which subsequently can be used for the evaluation of novel gene therapeutic strategies using a codon-optimized gp91phox transgene. We have used this strategy to test the potential of a novel gene therapy vector for X-CGD.

Molecular Therapy — Methods & Clinical Development (2014) **1**, 14037; doi:10.1038/mtm.2014.37; published online 27 August 2014

INTRODUCTION

Chronic granulomatous disease (CGD) is a rare inherited primary immunodeficiency characterized by a compromised immune system due to impaired neutrophil function. CGD often leads to premature death triggered by severe and therapy-resistant infections.[1] The antimicrobial activity of phagocytic cells mainly depends on the production of reactive oxygen species (ROS) by the nicotinamide dinucleotide phosphate (NADPH) oxidase enzyme complex. This complex consists of two membrane spanning subunits, gp91phox and p22phox, as well as three cytosolic components p47phox, p67phox, p40phox. In addition, the low-molecular-weight GTP-binding proteins Rac1 and Rac2 are also involved in the regulation of the NADPH oxidase activity.[2] CGD patients harboring genetic mutations in one of the subunits of the oxidase complex have a significantly reduced ROS production.[3] The X-linked form of the disease (X-CGD), which is caused by mutations in the X-linked gp91phox gene (*CYBB*) accounts for the majority (65–85%) of CGD cases.[4–6] The only curative treatment currently available is hematopoietic stem cell transplantation.[7,8] For those patients lacking a suitable donor, gene therapy of autologous hematopoietic stem cells (CD34+) is a promising alternative, as demonstrated in pioneering phase I/II clinical trials (as reviewed elsewhere).[9] Despite the undisputed clinical benefit experienced by all X-CGD subjects treated by gene therapy, the vector-related genotoxic effects observed in some of the patients clearly emphasized the development of safety and efficacy improved vectors (reviewed in ref. [10]). Consequently, novel retroviral vectors intended for clinical trials must be evaluated extensively

for safety and efficacy. The predictive values of these assays depend on the test systems used. For X-CGD a gp91phox deficient human myelomonocytic cell line (XCGD-PLB985),[11] is a valuable system for initial vector testing, however, it can only provide limited predictive data on clinical efficacy or safety. First, it is highly permissive for vector transduction in contrast to primary CD34+ HSCs and cannot give detailed insights in gp91phox expression kinetic during myeloid differentiation, e.g. for the evaluation of promoter regulation or studies on basic biology. Next, disproportional ROS production was previously shown for XCGD-PLB985 cells transduced with a gammaretroviral vector most likely due to defects in intracellular trafficking and maturation processes described for the parental cell line HL-60.[12,13] Furthermore, complete vector inactivation by epigenetic mechanisms was identified as one of the problems encountered in our Phase I/II clinical trial, a problem we never experienced in XCGD-PLB985 cells.[14,15] Hence, the best test system to evaluate vectors for gene therapy of X-CGD are primary CD34+ cells lacking gp91phox expression. However, for X-CGD, only minute amounts of patient derived primary material are available for research and thus, murine models of the disease are predominantly used for vector testing.[16] Besides the low incidence of the disease (1 in 120,000 to 1 in 250,000),[17,18] ethical considerations limit the availability of X-CGD CD34+ cells.

In an approach to overcome the acute paucity of primary human X-CGD cells, we developed a lentiviral vector for the stable knock-down of gp91phox in human primary hematopoietic stem cells from healthy donors. Efficient knock down of endogenous gp91phox

---

was achieved in PLB985 cells and in primary human CD34^{+} cells as assessed by FACS and western blot and resulted in loss of NADPH-oxidase activity closely matching the phenotype of X-CGD patient samples. These cells were used to test the efficacy of a novel lentiviral vector containing a codon-optimized version of gp91[phox]. Hence, this approach represents a valuable system for testing viral vectors in human primary X-CGD cells as well as for research focusing on the basic biology of gp91[phox].

RESULTS

Screening for optimal shRNAs and vector design for efficient gp91[phox] knock down

Initially, we tested five shRNAs individually in the context of a lentiviral vector for their activity to knock down endogenous gp91[phox] expression in the human myelomonocytic cell line PLB-985 (Figure 1a,b). Knock down efficiency of gp91[phox] expression was assessed in undifferentiated transduced cells and upon granulocytic differentiation by measuring gp91[phox] protein at the cell surface of transduced cells by flow cytometry using the human monoclonal anti-gp91[phox] antibody 7D5[19] (Figure 1c). Significant reduction of gp91[phox] positive cells was achieved with two shRNAs, sh88 and sh91 ($P < 0.001$ and $P = 0.002$, respectively), which were subsequently combined in a single lentiviral vector under the control of two distinct human DNA polymerase III promoters, namely U6 and H1. The insertion of the H1-sh91 sequence into the viral 3′ long terminal repeat (LTR) results in two transcription units per provirus upon reverse transcription (Figure 1d). This design led to the highest knock-down efficiency ($88 \pm 4\%$) in differentiated CD11b^{+} PLB-985 cells as estimated from gp91[phox] surface expression (Figure 1c). Clonal populations harboring 1–2 vector integrants confirmed gp91[phox] knock down at the mRNA level with a mean efficiency of $80 \pm 12\%$ ($n = 9$, Figure 1e). In this final knock down (KD) vector (LV.sh88/91.Cer, Figure 1d) a fluorescent marker gene, cerulean, allows the identification and sorting of KD-vector positive cells.
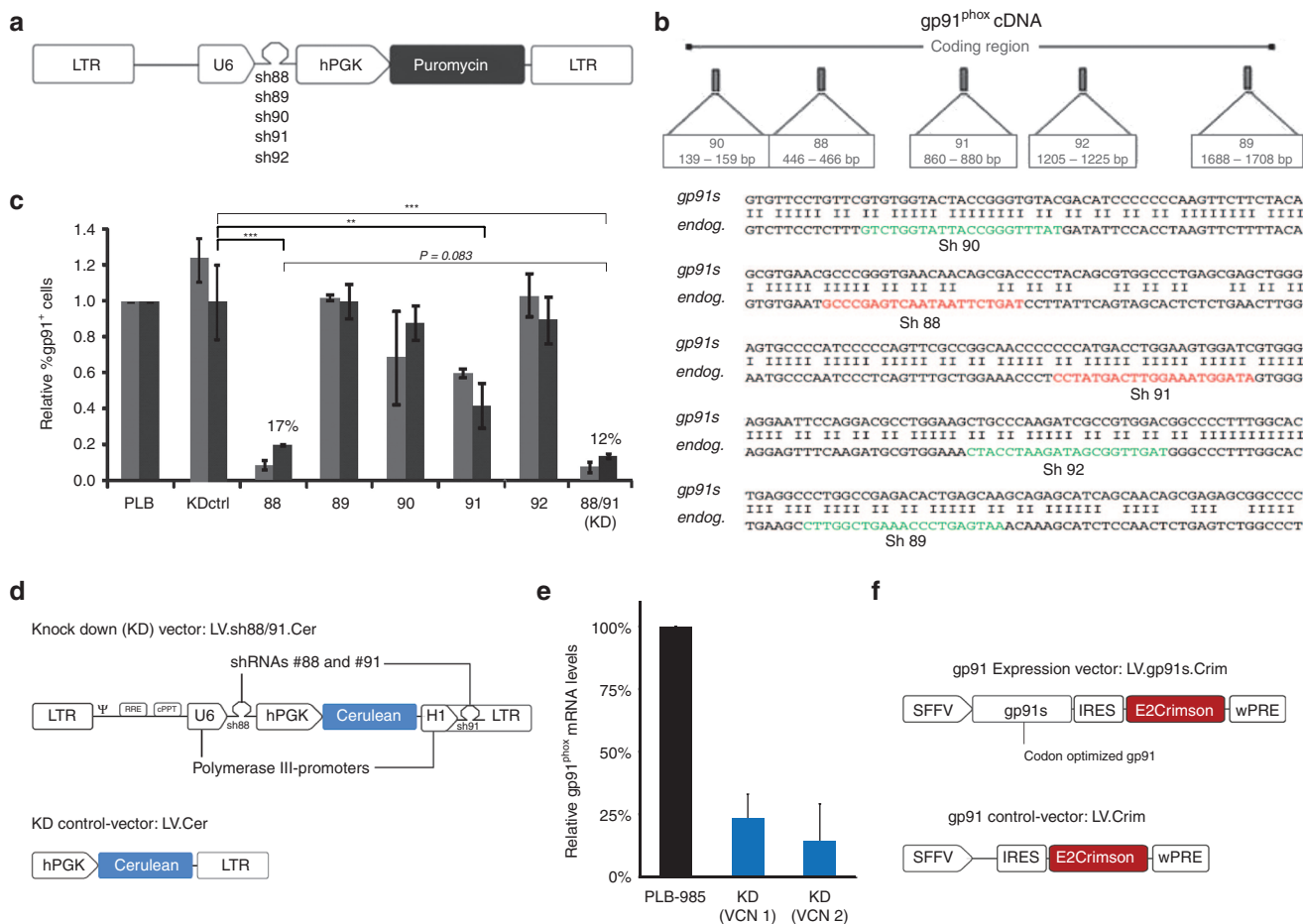

Figure 1 Screening of shRNAs for efficient knock down of gp91[phox]. (**a**) Schematic structure of lentiviral vectors tested for the knock down of gp91[phox] in PLB-985 cells. (**b**) Localization of the individual shRNA seeding sequences (colored in red and green) in the gp91[phox] coding region is shown aligned to the synthetic gp91s sequence. The best performers are highlighted in red. (**c**) PLB-985 cells were transduced with the shRNA vectors shown in **a** and 24 hours later subjected to puromycin selection for 4 days before gp91[phox] expression was analyzed in undifferentiated cells (gray) or in CD11b cells after granulocytic differentiation (>7 days, black bars). Gp91[phox] expression was normalized to non-transduced wild type cells (PLB-985). The gp91[phox] knock out cell line XCGD-PLB985 served as negative control ($n \geq 3$). (**d**) Plasmid configuration of the gp91[phox] KD (LV.sh88/91.Cer), and respective control-vector (LV.Cer) used in this study. (**e**) Quantitative RT-PCR was performed on single cell clones derived from KD-vector transduced PLB-985 cells to assess gp91[phox] knock down efficiency at the mRNA level. Clones were grouped according to vector copy number (VCN) as determined by qPCR (VCN 1: 1.1 ± 0.1, $n = 6$; VCN 2: 1.7 ± 0.1, $n = 3$). Expression was normalized to gp91[phox] mRNA expression levels of non-transduced PLB-985 cells and cDNA derived from XCGD-PLB985 served as negative control. (**f**) Schematic structure of the internal cassette used to reconstitute gp91 expression (LV.gp91s. Crim)) in knock down cells and the respective control vector (LV.Crim). cPPT, central polypurine tract; endog., endogenous sequence; hPGK, human phosphoglycerate kinase promoter; IRES, internal ribosome entry site; LTR, self-inactivating long terminal repeat; RRE, rev-responsive element; SFFV, spleen focus forming virus promoter; wPRE, woodchuck hepatitis virus posttranscriptional regulating element. Ψ Packaging signal. Error bars = SD.

## shRNA-mediated knock down of gp91[phox] and rescue of gp91[phox] expression in a myeloid cell line

LV.sh88/91.Cer transduced PLB-985 cells were tested for re-expression of gp91[phox] from a lentiviral vector containing a codon-optimized version of the gp91[phox] cDNA, gp91s.[20] This vector contained in addition a fluorescence marker, E2-Crimson, to distinguish re-expression from wild type gp91[phox] expression in non-transduced cells (LV.gp91s.Crim, Figure 1f). After transduction and granulocytic differentiation four distinct populations could be distinguished by FACS analysis (Figure 2a). Cerulean-positive cells (upper left quadril in Figure 2a) identified a population of CD11b^{+} PLB-985 cells lacking gp91[phox] expression (KD-cells), while non-transduced (ntd) cells were identified by the lack of fluorescence marker expression (lower left quadril). Gp91s expressing cells were visualized by E2-Crimson expression (lower right quadril) while double transduced cells with knock down of endogenous gp91[phox] and re-expression of gp91s were identified by the combination of Cerulean and E2-Crimson fluorescence (upper right quadril in Figure 2a). Although PLB-985 can be efficiently transduced with these vectors according to marker expression (>90%, data not shown), moderate transduction rates (<50%) combined with FACS sorting were preferred to control for low vector copy number. After FACS sorting of the individual cell populations, expression of gp91[phox] was reanalyzed by FACS and western blotting (Figure 2b,c). This analysis included non-transduced PLB-985 cells as well as XCGD-PLB985 cells. As expected, gp91[phox] protein was absent from XCGD-PLB985 cells as well as from KD cells and clearly visible in non-transduced PLB-985 cells and in PLB-985 cells transduced with a control vector (LV.Cer) expressing only Cerulean. Most importantly, gp91[phox] protein was detectable at wild type levels in KD cells transduced with the gp91 re-expression vector LV.gp91s.Crim, confirming that re-expression of a codon-optimized gp91[phox] is feasible in the background of shRNAs targeting the wild type version of gp91[phox] (Figure 2c).

Next, we stimulated the cells with phorbol-12-myristate-13-acetate (PMA) to test for oxidase activity in KD- and LV.gp91s.Crim double transduced PLB-985 cells. NADPH oxidase activity was assessed by superoxide production over time using the cytochrome C reduction assay.[21] Only residual oxidase activity (0.16 nmol superoxide/minute $\times 10^6$ cells) was detected in KD cells, closely matching the values observed in XCGD-PLB985 control cells thereby reflecting the X-CGD phenotype. As expected from the expression data, LV.gp91s.Crim restored superoxide production in KD cells to wild type levels (2.36 versus 2.33 nmol superoxide/minute $\times 10^6$ cells, respectively; Figure 2d). Therefore, the X-CGD phenotype can be efficiently mimicked by introducing the LV.sh88/91.Cer vector into wild type PLB-985 cells as estimated by biochemical and functional assays. Functionality can be restored in these cells after transduction with LV.gp91s.Crim.

Knock down approach mimics functional the X-CGD phenotype in CD34^{+} derived human cells

We used granulocyte-colony stimulating factor (G-CSF) mobilized peripheral blood from healthy donors to establish a surrogate model for primary human X-CGD cells. Thus, we first analyzed whether the introduction of the knock down vector in CD34^{+} cells reduces or even abrogates ROS production in their *in vitro* differentiated myeloid progeny (CD11b^{+}) upon PMA stimulation. After CD34^{+} cell isolation

shRNA-generated X-CGD cells for vector analysis
C Brendel et al.

4

b
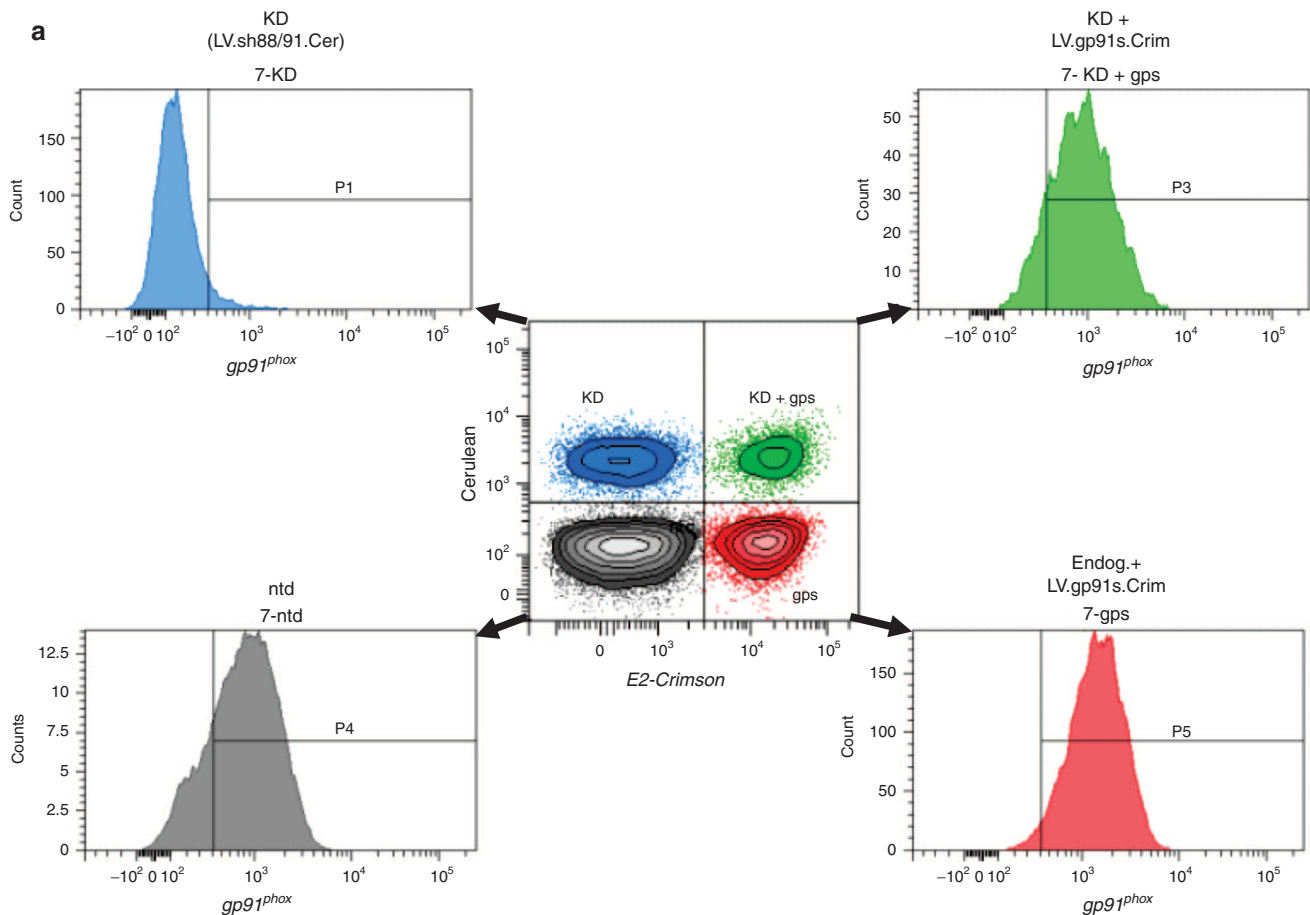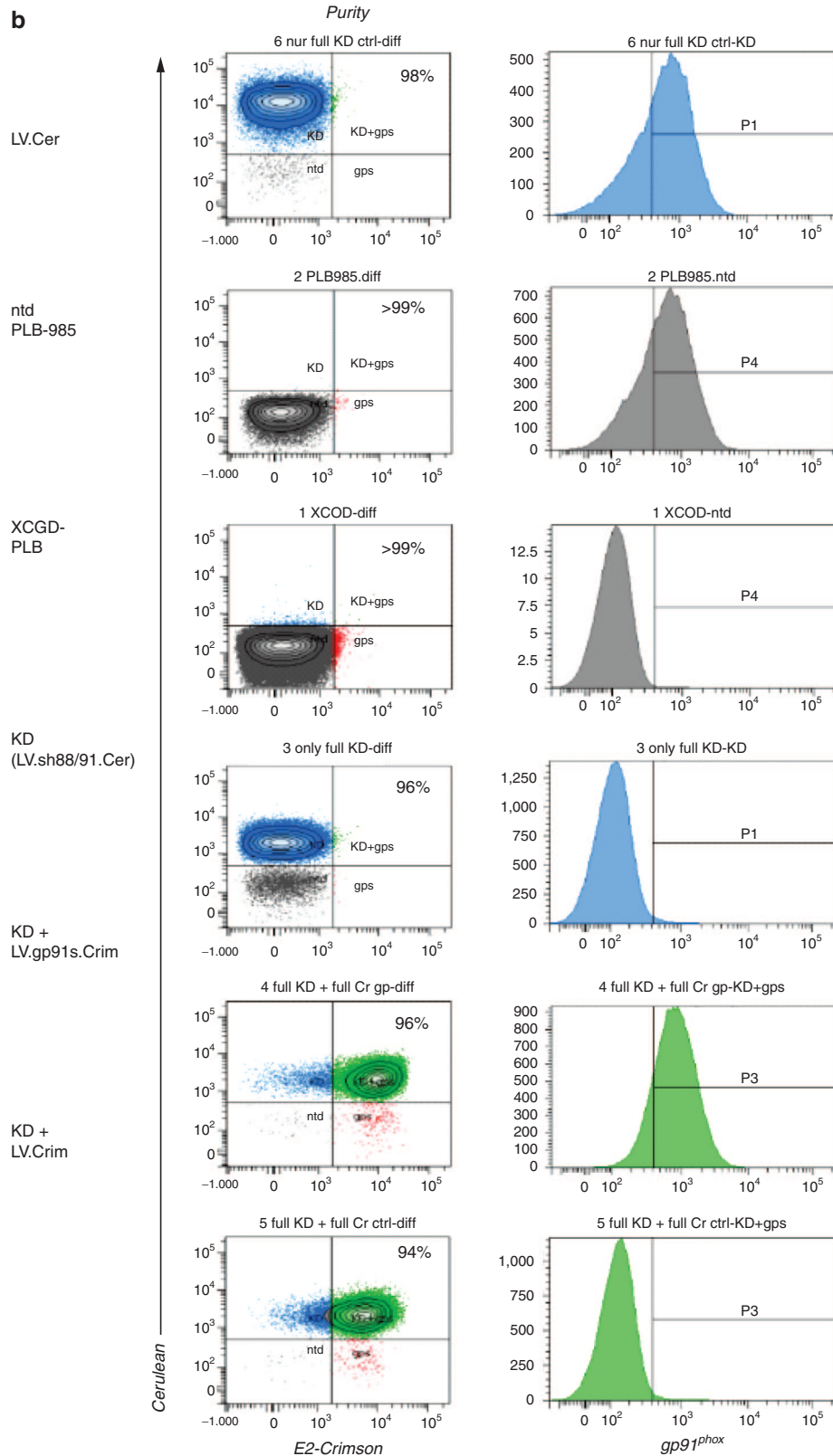
cells were pre-stimulated for 1 day before transduction with the LV.sh88/91.Cer. After transduction prolonged *in vitro* culture (2–3 weeks) in the presence of human G-CSF was required for full granulocytic maturation and optimal gp91phox expression. After sorting for Cerulean+ cells CD11b+ cells derived from KD transduced CD34+

cells revealed only background staining in the nitroblue-tetrazolium (NBT)-reduction assay, similar to the staining obtained with myeloid progeny derived from X-CGD CD34+ cells (Figure 3a). In contrast, wild type CD11b+ cells demonstrated oxidase activity as indicated by the reduction of NBT to insoluble formazan in the majority of the cells as

documented by a dark blue deposit on the cells (Figure 3a). This observation was further confirmed by the quantitative cytochrome C assay, in which only residual superoxide production (12.7% of wt) could be measured in the CD11b+ KD-cells (Figure 3b,c) roughly mimicking the complete absence of superoxide production we had observed previously in XCGD-CD34+ derived cells.[18,22] We also used the dihydrorhodamine123 (DHR123) assay to detect ROS produced by KD-, X-CGD and normal phagocytes after PMA stimulation. Cerulean expressing cells showed only residual rhodamine123 (Rho123) staining suggesting minimal superoxide production by these cells, similar to samples derived from X-CGD patients (Figure 3d). Thus, the LV.sh88/91.Cer vector efficiently induced the X-CGD phenotype in primary CD34+ cells proving the applicability of our knock down strategy to generate a surrogate human model of X-CGD.

Stable knock down and rescue of gp91phox expression and functional activity in human primary cells

Next, we assessed if our KD-vector induced human model of X-CGD in HSCs allows for the functional evaluation of gene therapy vectors. Again, prestimulated CD34+ cells were transduced either with the KD- or LV.Cer vector and in addition with LV.gp91s.Crim or the respective control vector LV.Crim (Figure 1d,f). After transduction and granulocytic differentiation roughly 70% of the cells stained positive for the CD11b myeloid cell surface marker and from these only 3.4% of the LV.sh88/91.Cer transduced, Cerulean positive cells (KD-CD34+ cells) showed residual gp91phox expression at low levels when compared to gp91phox expression levels in Cerulean negative, wild type cells (Figure 4a, upper panels and Figure 4b). Thus, more than 95% of the KD-vector transduced cells lacked gp91phox expression. Transduction of the KD-CD34+ cells with LV.Crim did not alter the gp91phox expression pattern (Figure 4a, middle panels). In contrast, transduction of the KD-CD34+ cells with LV.gp91s.Crim resulted in 25–35% total transduction efficiency as determined by E2-Crimson expression by FACS with almost 100% of the E2-Crimson positive cells expressing gp91phox (Figure 4a, lower panels). The levels of re-expression even exceeded gp91phox expression by wild type cells (Figure 4b). Thus, gp91phox expression can be efficiently reduced (11.1-fold, $P = 0.0099$; Figure 4b) and rescued in myeloid (CD11b+) cells after gene transfer into primary human CD34+ cells using the strategy outlined here. As expected, re-expression of gp91phox also rescued the functional X-CGD phenotype of our model as demonstrated by ROS production in CD11b+ double transduced cells (KD- and LV.gp91s.Crim) according to the DHR assay (Figure 4c). Hence, the delivery of LV.gp91s.Crim into the KD-CD34+ cells resulted in re-expression of gp91phox and functional rescue of the X-CGD phenotype proving the applicability of our knock down strategy for the functional evaluation of gene therapy vectors.
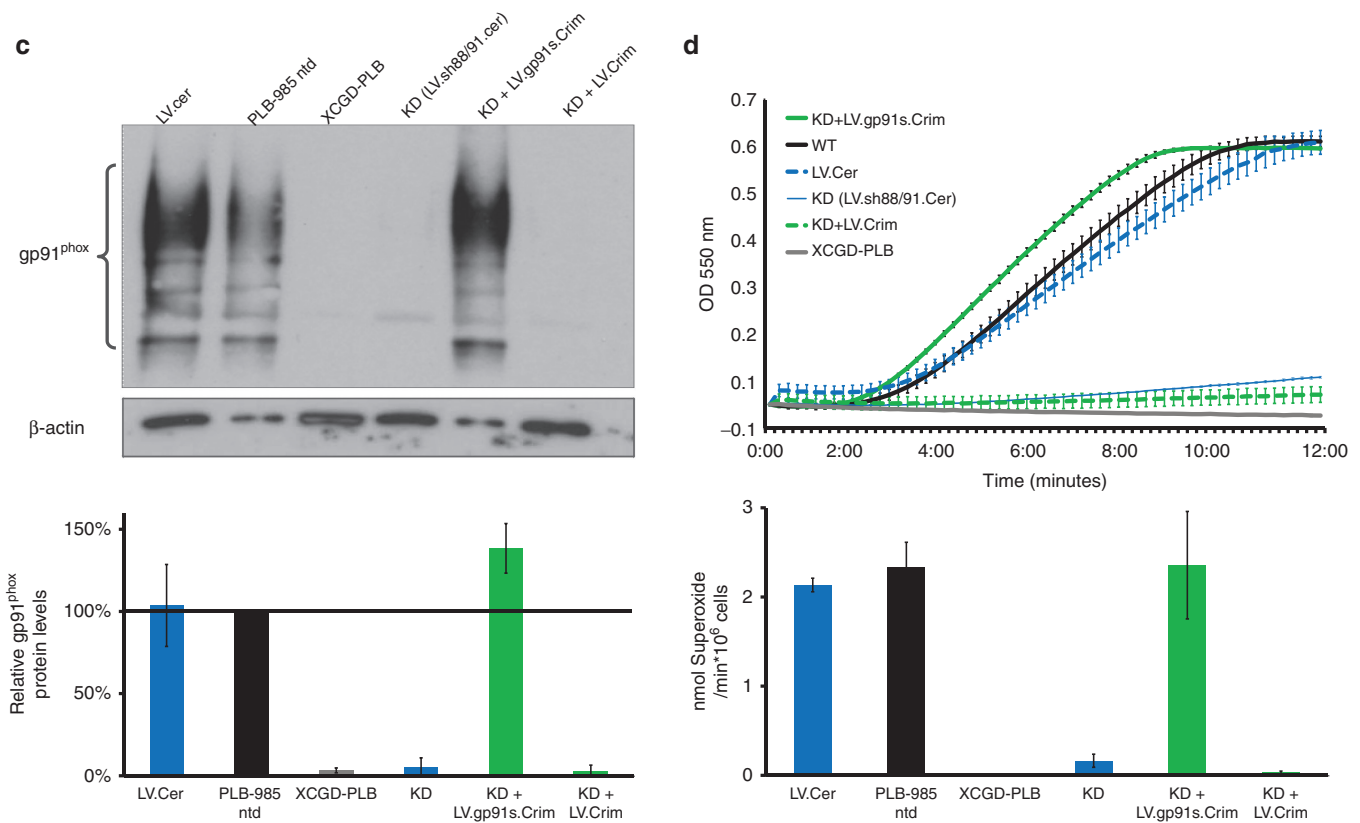

Figure 2 Knock down and re-expression of gp91phox in PLB-985 cells. (**a**) Representative FACS plots demonstrating the gating strategy used for the analysis of shRNA-treated cells and after re-expression of gp91s. PLB-985 cells were transduced with the lentiviral vectors shown in Figure 1d,f. Cells were stained for gp91phox expression 5 days after transduction. Cell populations were identified according to the fluorescent markers co-expressed by the vectors as follows: wild type gp91phox expression levels, gray; knock down of gp91phox expression, blue; re-expression of gp91s, red, double-transduced cells green. (**b**) Re-analysis of cell populations after FACS-sorting for the respective fluorochromes to evaluate purity and gp91phox expression in the individual cell populations. (**c**) Sorted cells were subjected to western blot analysis to detected the highly glycosylated gp91phox protein. β-actin was used as reference. Normalized gp91phox expression levels obtained from three individual experiments are given in a bar representation below. Ratio of gp91phox to β-actin in non-transduced PLB-985 cells was set to 100% and XCGD-PLB985 cells lacking gp91phox expression served as negative control. (**d**) ROS production was determined in transduced cells by the cytochtome C reduction assay upon PMA stimulation of myeloid differentiated cells over time in triplicate. The bar chart below summarizes the results of three independent experiments. Error bars = SD.

Evaluation of a clinical vector for restoration of gp91[phox] expression in KD-induced primary X-CGD cells

In a final proof of principle experiment we tested a lentiviral vector (ChimGp91)[23] used in an ongoing multicentric clinical trial (NCT01855685/ www.clinicaltrials.gov) that is devoid of a fluorescent marker gene in our novel primary cell test system. Within this vector gp91s expression is regulated by a chimeric myeloid specific promoter composed of sequences derived from the Cathepsing G and the c-FES regulatory genomic regions and thus targets transgene expression to mature myeloid cells (Figure 5b). CD34^{+} cells were transduced with the KD-or LV.Cer vectors as before and subsequently transduced with ChimGp91, LV.Crim or left untransduced. Again, efficient reconstitution of gp91[phox] expression (44.8%) was demonstrated following *in vitro* differentiation with expression levels in the range of nontransduced (wild type) cells, similar to the results obtained upon transduction of patient-derived X-CGD CD34^{+} cells with this particular vector[23] (Figure 5a,b). Hence, KD-vector transduced CD34^{+} cells can be used for the evaluation of transduction efficiency and expression properties of therapeutic vectors and monitor correction of the X-CGD disease phenotype. In addition, KD-vector transduced CD34^{+} cells were able to engraft NSG mice as demonstrated by 9.0±4.7% (*n* = 6) of the human CD45^{+} cells expressing Cerulean 8 weeks after transplantation (Figure 5c,d).

DISCUSSION

We achieved an almost complete knock down of endogenous gp91[phox] expression in mature myeloid cells derived from PLB-985 and CD34^{+} cells via shRNA-mediated degradation of endogenous gp91[phox] transcripts, resulting in the lack of gp91[phox] surface expression in 88% to 96% of LV.sh88/91.Cer transduced cells. Using a codon-optimized version of gp91[phox], which is not recognized by the shRNA, we reconstituted gp91[phox] expression and NADPH-oxidase function in these cells. In our study we used two lentiviral vectors each co-expressing a distinct fluorophore to label cells transduced with the shRNA and/or the gp91s re-expression vector. This approach facilitate the tracing of untransduced, single or double transduced populations by FACS or fluorescence microscopy and therefore allows for the monitoring of essential controls within the mixed cell population of transduced and untransduced cells. Thus, we normalized the degree of gp91[phox] downregulation to the levels of gp91[phox] expression in the untransduced fraction of cells in the same experiment. Similarly, double-transduced cells expressing both, the shRNA and gp91s, were identified by the combination of both fluorochromes. Using this strategy we could compare the expression levels of gp91s to the endogenous gp91[phox] levels in one single FACS analysis as represented in Figure 4a middle panel. The alternative approach, which is to integrate shRNA and gp91s in one vector backbone, would not allow for the analysis of the individual populations separately nor for preclinical vector testing and therefore was not considered for our studies. The high and sustained knock down of gp91[phox] expression by LV.sh88/91.Cer vector in CD34^{+} derived cells (>95% depletion of gp91[phox] surface expression) allowed us to test a clinical vector lacking a reporter marker for the identification of transduced cells. Gp91s expression levels from the ChimGp91 vector were lower than wild type levels but still within the therapeutic range as demonstrated previously by us in a series of functional analysis.[23]

Our system bypasses the lack of patient derived X-CGD CD34^{+} cells and is also of potential interest for researchers investigating the basic biology of gp91[phox] and NADPH-oxidase function. Our knock–down strategy in CD34^{+} cells may also provide insights into the role of gp91[phox] in stem cell physiology, as primary cells lacking gp91[phox] seem to be actively cycling (data not shown). The consequences of

this observation need to be analyzed in detail but may explain at least in part the lack of long-term engraftment observed in gene therapy trials for XCGD and also may addressed safety issues as a series of cell cycle regulators may be active in gp91[phox]-deficient primary cells which could serve as target for vector integration. Consequently integrome analysis of transduced and engrafted gp91[phox]-deficient CD34^{+} cells could provide information on the potential genotoxic effects associated with the use of integrating vectors in CGD.[10] For all these reasons, we believe that disease-specific tools are fundamental to predict the outcome of gene transfer into primary cells. This may be specific for CGD, but it would be worthwhile to implement similar knock-down strategy for other diseases for which primary material is not routinely available.

As an alternative to our approach, induced pluripotent stem cells (iPSCs) have been derived from a large number of normal and defective somatic tissues and have been used to gain insight into the molecular basis of diseases, for testing therapeutic approaches and for drug screenings. Human X-CGD iPSCs have been generated from mesenchymal stem cells derived from bone marrow aspirate of a patient and have been used to correct the disease by Zn-finger nuclease mediated targeting of a gp91[phox] transgene into the AAVS1 gene locus.[24] However, transplantable HSCs derived from iPSCs would be the desired cell type for the *ex vivo* testing of gene therapy vectors and optimization of transduction protocols. Although several reports have described the induction of hematopoietic progenitors from human iPSCs or human embryonal stem cells, the generation of hematopoietic cells with long-term and multilineage engraftment potential has not yet been achieved.[25–32] In contrast to the sophisticated protocols used for the generation of iPSCs and the subsequent derivation of hematopoietic cells, our shRNA approach could theoretically be performed as a one-step procedure, as both vectors can be mixed before transduction of CD34^{+} cells generating a surrogate transplantable disease model within 2–3 days while using the same cell source as in clinical gene therapy protocols.

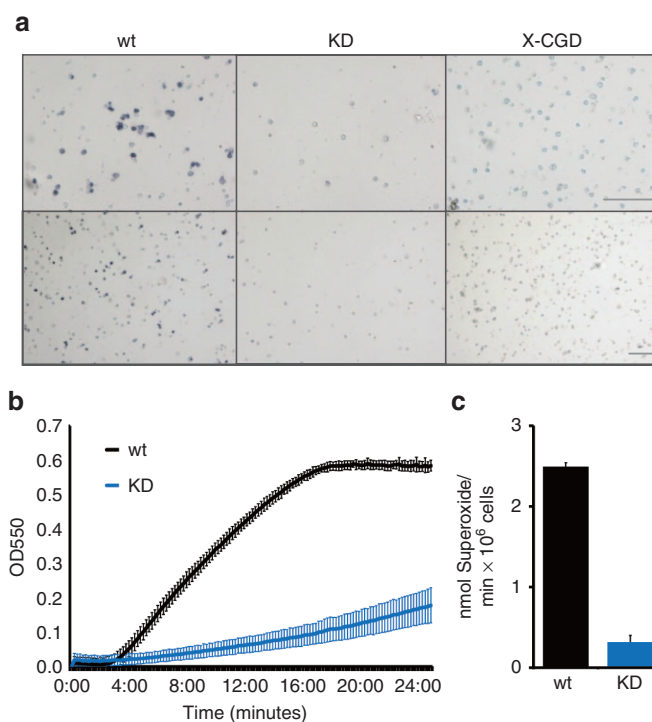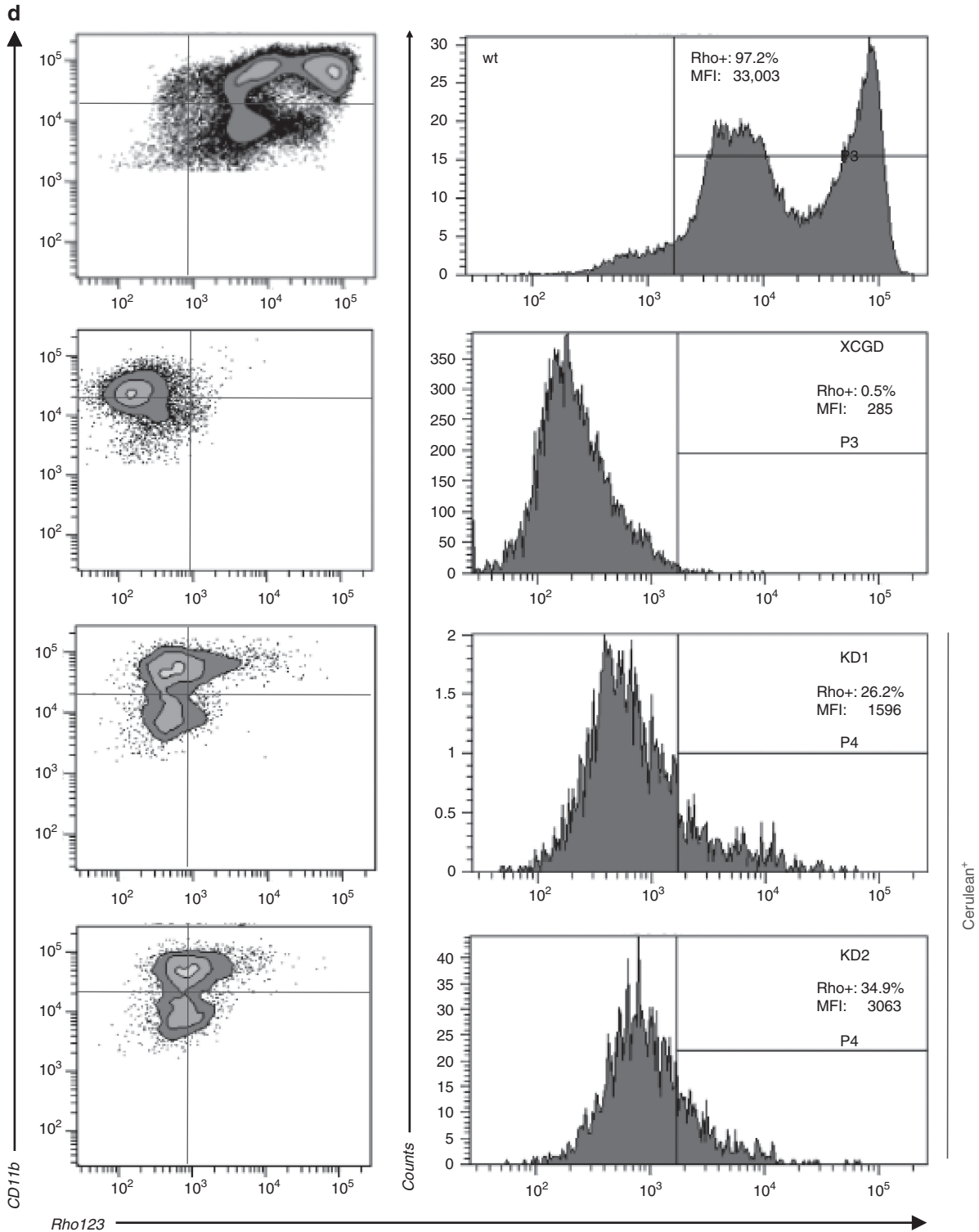**Figure 3** Continued on next page.

shRNA-generated X-CGD cells for vector analysis
C Brendel et al.

7

Figure 3 NADPH oxidase activity upon gp91phox knock down in human CD34+ HSC derived cells. LV.sh88/91.Cer transduced CD34+ cells were subjected *to in vitro* granulocytic differentiation and FACS-sorted for Cerulean expression (purity: 90.0±2.5%, *n* = 3) prior to oxidase activity measurements. (**a**) Oxidase activity was visualized in differentiated cells after PMA stimulation by the Nitro-Blue-Tetrazolium (NBT). Superoxide producing cells are visualized by a dark blue formazan deposit. Nontransduced cells were used as positive control while cells derived from a X-CGD sample served as negative control. Two magnifications of the same samples are shown (scale bar = 100 μm). (**b,c**) Cytochrome C assay was performed and values were corrected for purity after FACS sorting. (**d**) A dihydrorhodamine (DHR) assay was performed with unsorted populations after transduction and myeloid differentiation of CD34+ cells. Oxidation of dihydrorhodamine 123 to rhodamine 123 is shown for non-transduced wild type (wt), CD34+X-CGD patient sample derived cells (XCGD) and two Cerulean+ cell populations after transduction with LV.sh88/91.Cer (KD1, KD2). Included in the histograms are the fraction of superoxide producing (Rho+) cells, and the mean fluorescence intensity (MFI) of gp91phox protein expression in CD11b+ cells.

Although shRNA-mediated disruption of gene function has been broadly evaluated for therapeutic applications (as reviewed elsewhere),[33] disease modeling of a monogenetic disorder by RNA-interference and subsequent rescue has been only demonstrated for Fanconi anemia using human embryonal stem cells (hESC).[34] However, in this case, overexpression of the therapeutic gene was used to overcome siRNA-mediated downregulation. Hence, we provide the first disease modeling in CD34+ cells by shRNA that in addition can be rescued by delivering a synthetic sequence of the targeted gene. This concept is promising for other rare monogenetic diseases in focus of gene therapy, since codon-optimized transgenes are widely used in current gene therapy approaches and their evaluation is usually hampered by low availability of patient derived samples.[9,35–37] Recent progress in designer nuclease approaches, such as zinc-finger and TALE nucleases as well as more recent the CRISPR/Cas9 system, offer the possibility of a true genetic knock out. However, their wide application is still hampered by low efficiency of gene disruption and delivery of the nucleases into CD34+ cells.[22,38,39]

In conclusion, we provide a straight forward approach to overcome the paucity of X-CGD CD34+ cells by using a lentiviral mediated gp91phox knock down vector that efficiently abrogates gp91phox expression as well as NADPH oxidase activity in the myeloid progeny. This surrogate primary X-CGD model enables the evaluation of novel vectors for X-CGD gene therapy in terms of transduction efficiency of CD34+ cells, gp91phox expression levels and oxidase activity in order to ultimately estimate if a therapeutic benefit can be anticipated upon clinical application of the vector tested. Furthermore, the simplicity of this approach allows its implementation in nearly every laboratory working with lentiviral vectors and with access to primary CD34+ cells. Lastly, the potential applicability of our test system extends beyond gene therapy as it is an ideal model to shed further light on the role of gp91phox, NADPH oxidases and ROS-production in hematopoietic stem cell biology.

MATERIALS AND METHODS

Lentiviral vectors and vector production

Commercially available lentiviral transfer plasmids (pLKO.1) harboring shRNAs #64588-#64592 (Sigma-Aldrich, Steinheim, Germany) were used for initial experiments and served for further downstream cloning. The Cerulean sequence was excised from pLeGO-Cer (Addgene plasmid #27351) using the restriction sites for *BamHI* and *EcoRI*, blunted and inserted in pCR2.1-TOPO (Life Technologies, Karlsruhe, Germany) to obtain flanking *BamHI* and *NsiI* sites to cut and insert it into *BamHI* and *NsiI* digested pLKO.1 plasmid replacing the puromycin resistance gene. The thereby obtained pLKO.sh88.PGK.cer was subsequently subjected to *NdeI* and *EcoRI* digestion followed by religation and resulting in pLKO.PGK.cer (LV.Cer).

Following manufacturer's protocol, shRNA91 obtained by annealing of two oligonucleotides (sense: 5′-GATCTCCGGCCTATGACTTGGAAA
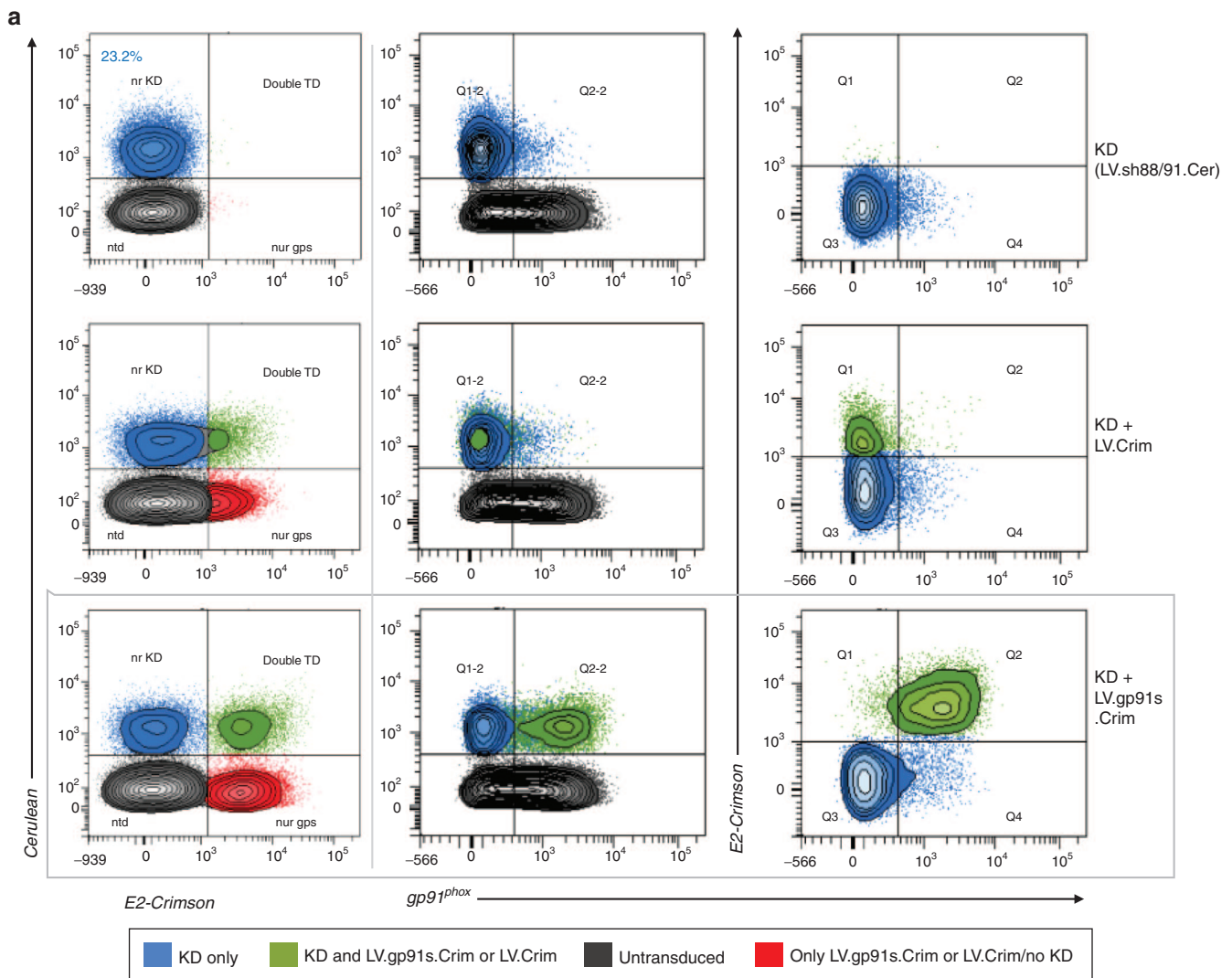
TGGATACTCGAGTATCCATTTCCAAGTCATAGGTTTA-3', antisense: 5'-AGCTTC AAAAACCTATGACTTGAAAATGGATACTCGAGTATCCATTTCCAAGTCATAGGCC GG-3') was cloned into the pSupervector (OligoEngine, Seattle, WA) harboring the H1 promoter using *BglII* and *HindIII*. The H1-shRNA91 cassette was then excised by *EcoRI* and *KpnI* digested, blunted and cloned into the *BbsI* restriction site within the 3'LTR of pLKO.sh88.PGK.cer resulting in the final KD-vector (LV.sh88/91.Cer) plasmid.

E2-Crimson from the pE2-Crimson plasmid (Clontech Takara Bio, Saint-Germain-en Laye, France) was inserted into pHR'.SFFV.IRES.GFP.wPRE[40] by the use of *NcoI* and *SpeI* sites in both plasmids, resulting in the gp91control vector pHR'.SFFV.IRES.E2Crimson.wPRE (LV.Crim). The codon-optimized gp91[phox] cDNA (gp91s) was PCR amplified from the original PCRscript-gp91s plasmid obtained from GeneArt (Life Technologies)[20] inserting flanking *SacII* restriction sites (forward primer: 5'-CCGCGGATCCGACCGATCCTGCCACCATG-3';
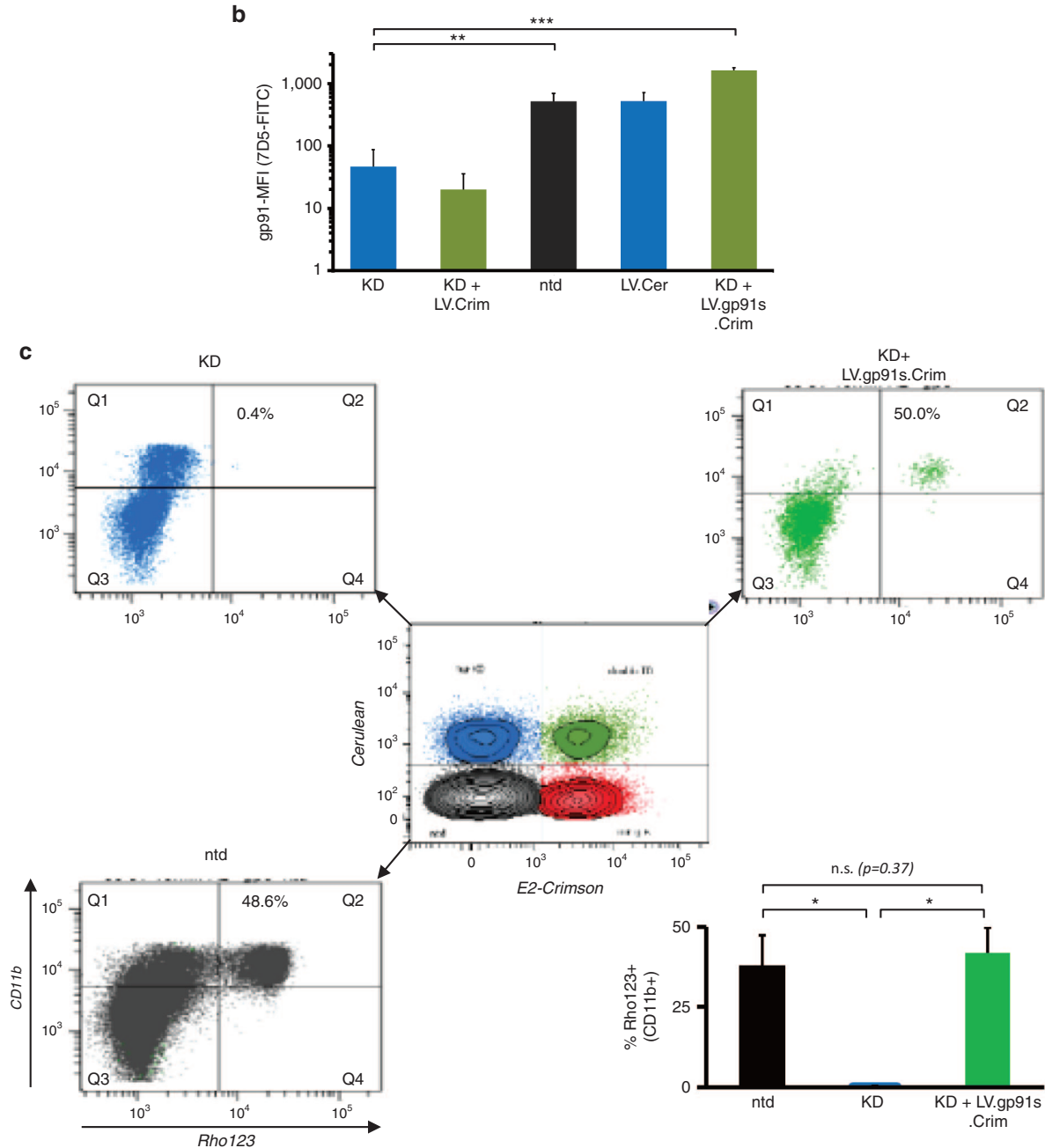

Figure 4 Knock down, re-expression of gp91[phox] and functional rescue of gp91[phox] activity in CD34^{+} HSC derived cells. (**a**) Mobilized peripheral blood CD34^{+} cells were transduced with the indicated vectors or vector combination further expanded for 6 days and subsequently subjected to granulocytic differentiation (2–3 weeks). The same gating strategy as described in Figure 2a was applied on viable CD11b^{+} myeloid cells. Upper panels: Transduction and gp91[phox] expression in CD34^{+} cells transduced with LV.sh88/91.Cer (blue). Middle panels: Transduction and gp91[phox] expression in CD34^{+} cells transduced with LV.sh88/91.Cer (blue) and LV.Crim (red). Lower panels: Transduction and gp91[phox] re-expression in CD34^{+} cells transduced with LV.sh88/91.Crimvector (red). The green fluorescence marker denotes the proportion of cells containing both vectors. The outcome of the experiment is summarized in). (**c**) Oxidase activity according to the dihydrorhodamine (DHR) assay is shown for nontransduced (ntd), KD vector only and KD vector and LV.gp91s.Crim transduced cell populations and summarized in the lower right panel (*n* = 3). Percentages given refer to the Rho123^{+} cells within the CD11b^{+} cell fraction. ctrl, control, MFI, Mean fluorescence intensity, 7D5-FITC: FITC conjugated monoclonal murine antibody against human gp91[phox]. Error bars = SD, *P < 0.05, **P < 0.01, ***P < 0.001.

shRNA-generated X-CGD cells for vector analysis
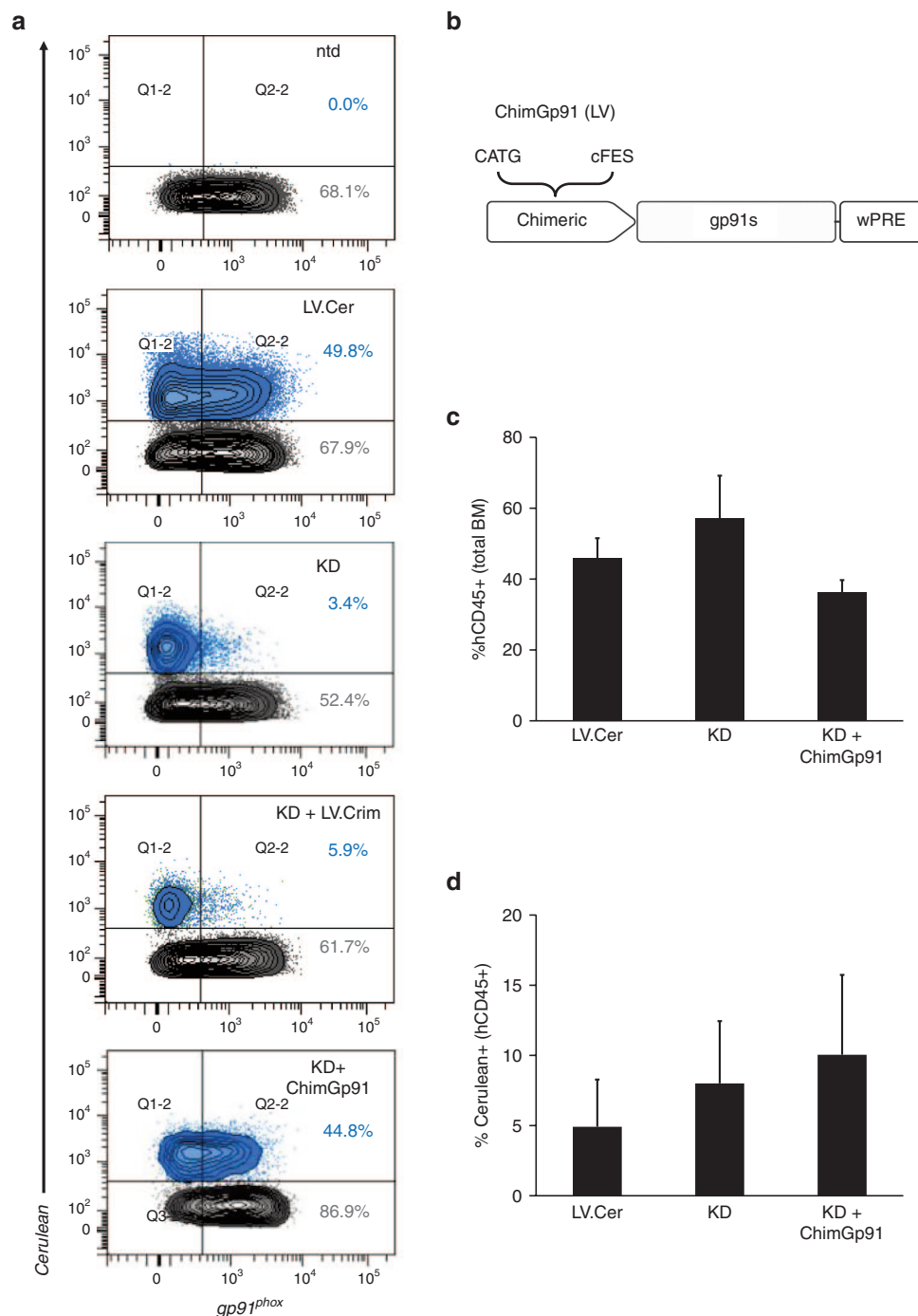C Brendel et al.

10

Figure 5 Evaluation of the clinical vector ChimGp91 in shRNA-derived CD34+X-CGD cells. (**a**) CD34+ cells were transduced with the KD-vector and the lentiviral vector ChimGp91 or control vectors (LV.Cer, LV.Crim). After 6 days of expansion and 14 days of *in vitro* differentiation towards granulocytes, gp91phox expression was measured by flow cytometry. Representative FACS plots show gp91phox and Cerulean expression in CD11b+ cells. Percentage values given indicate either gp91phox expression among the Cerulean-positive (blue) or negative fraction (gray). (**b**) Schematic representation of the internal cassette of the clinical lentiviral vector (LV) ChimGp91. The chimeric promoter is composed of sequences derived from the human Cathepsin G (CATG) and the human c-FES promoter. (**c,d**) CD34+ cells transduced with the indicated vectors (LV.Cer, KD, KD and ChimGp91) were transplanted into NSG mice (n = 2–3) and 8 weeks later the extent of (**c**) human hematopoietic (hCD45+) and (**d**) Cerulean+ cell engraftment was assessed. Error bars = SD.

reverse primer: 5′-CCGCGGGTCATCAGAAGTTTTCTTTGTTGAAGATG-3′) and the amplicon was subcloned into pCR2.1-TOPO. Following SacII digestion gp91s was inserted into the gp91control vector generating pHR′.SFFV. gp91s.IRES.E2Crimson.wPre (LV.gp91s.Crim). All restriction enzymes were purchased from NEB (Schwalbach, Germany).

Transient co-transfection on HEK293T cells was used to generate cell-free viral supernatants. Briefly, transfer vectors, lentiviral gag/pol helper plasmid and envelope plasmid pMD2.VSV.G (Addgene plasmid 12259: pMD2.G)

encoding the glycoprotein of vesicular stomatitis virus (VSV-G) were transfected in a molar ratio of 3:1:1 by the polyethylene imine (PEI) precipitation method according to standard procedures. Fourty-eight hours post transfection viral supernatants were harvested and sterile filtered (0.45 μm pore-size PVDF-membrane filter; Millipore, Schwalbach, Germany) and concentrated (60- to 100-fold) by ultracentrifugation over a 20% (w/v) sucrose cushion (50,000g, 2 hours, 4 °C). Pelleted vector particles were resuspended in StemSpan SFEM serum-free medium (StemCell Technologies, Grenoble,

shRNA-generated X-CGD cells for vector analysis
C Brendel et al.

11

France) without any supplements stored at −80 °C. Vector titers were determined in serial dilutions of viral supernatant by transduction of PLB-985 cells, analyzed 4–5 days after transduction by flow cytometry (BD FACSCanto II, BD FACSDiva 6.1.3 software, Becton Dickinson, Heidelberg, Germany) and were in the range of 10^8–10^9 TU/ml.

Cell lines and culture conditions

The human PLB-985 myelomonocytic leukemic cell line and its derivative XCGD-PLB985 (XCGD-PLB), in which the *CYBB* gene encoding for gp91[phox] was disrupted by homologous recombination[11] were grown in RPMI 1640 (Gibco/ Life Technologies) complemented with 10% heat-inactivated fetal calf serum (FCS; PAN-Biotech, Aidenbach, Germany), 4 mmol/l L-glutamine and antibiotics (100 U/ml penicillin and 100 µg/µl streptomycin; all from Gibco) in the presence or absence of 4 µg/ml puromycin. HEK293T cells (ATCC) were cultured in Dulbecco's modified Eagle's medium (Gibco) with identical supplements as stated above. PLB-985, XCGD PLB-985 and derivatives were cultured at a density of 2×10^5 cells/ml in RPMI 1640 supplemented with 2.5 % heat inactivated FCS, 4 mmol/l L-glutamine, 100 U/ml penicillin, 100 µg/µl streptomycin and 1.25% dimethyl sulfoxide (Sigma-Aldrich) for at least 7 days to induce granulocytic differentiation. Expression of the marker gene CD11b was used to verify differentiation status (flow cytometry).

Isolation, culture, and transduction of human CD34+ cells

Human CD34-positive cells from G-CSF mobilized peripheral blood of healthy donors were freshly purified using the human CD34 Microbead Kit (MiltenyiBiotec GmbH) according to manufacturer's instructions. For expansion cells were cultured in StemSpanSFEM (StemCell Technologies), 1% penicillin-streptomycin, hSCF (50 ng/ml), hTPO (10 ng/ml), hIGFBP2 (100 ng/ml) and hFLT3L (50 ng/ml).[41] Following overnight pre-stimulation cells were lentivirally transduced at a mulitplicity of infection of 20–50 with the vector input not exceeding 20% of the total cell culture volume. Therefore, cells were plated at a density of 1×10^6 cells per ml in 96- to 24-well-plate format. Half medium exchange was performed after overnight incubation, and in some cases a second round of transduction was performed to introduce the re-expression vector. Cells were further expanded under the same cytokine conditions for 3 days before granulocytic differentiation was initiated by adding 50 ng/ml hG-CSF to the media. To obtain terminally differentiated granulocytes the cells were thoroughly washed with PBS and cultured in IMDM (Lonza) supplemented with 20% heat-inactivated FCS, 4 mmol/l L-glutamine and antibiotics (1% penicillin-streptomycin) in the presence of 50 ng/ml hG-CSF for 2–3 weeks. All cytokines were purchased from Peprotech (Hamburg, Germany). The local Ethics Review Board of the University of Frankfurt Medical School approved the use of these cells and informed consent was obtained in accordance with the Declaration of Helsinki.

Flow cytometry

For flow cytometric analysis cells were washed and resuspended in PBS and unspecific Fc-binding was blocked by the addition of FcR blocking reagent (Miltenyi Biotech). The added antibodies for surface staining were: Fluoresceinisothiocyanate (FITC)-conjugated murine anti-human gp91[phox] monoclonal 7D5 ("7D5-FITC", MBL international no. D162-4), CD34-APC(4H11), anti-human CD45-PerCP-Cy5.5 and either CD11b-APC or CD11b-PE-Cy7 conjugates (all eBiosciences, Frankfurt, Germany). Use of the fixable viability dye eFluor 780 (eBioscience) supported dead cell exclusion. After 20–30 minutes incubation at room temperature in the dark, cells were washed and resuspended in PBS. Data acquisition was performed on a BD FACSCanto II and FACS sorting on a BD FACSAria flow cytometer. For data analysis FACSDiva 6.1.3 software (Becton Dickinson, Heidelberg, Germany) was used.

Quantitative reverse transcription PCR

Total RNA was extracted from 10^6 transduced PLB-985 clonal populations using the RNAqueous-Micro Kit with subsequent DNAase treatment (Ambion, Darmstadt, Germany) according to the manual. Next, 1 µg of RNA was subjected to reverse transcription with random primers applying the RETROscript Kit (Ambion) following manufacturer's instructions. Thereby generated cDNA (2.5 µl) was analyzed by quantitative reverse transcription PCR (qRT-PCR) using the LightCycler480 SYBR Green MasterMix following standard procedures on a LightCycler480 device (Roche, Mannheim, Germany). Quantification was facilitated by a standard curve using cDNA of nontransduced PLB-985 cells. GAPDH served as reference gene. Primer were as follows: Gp91 for: 5′-GGTTTTGGCGATCTCAACAGAA-3′; Gp91 rev: 5′-TTCAAAATGGAAGTGGGACAATACA-3′; GAPDH for: 5′-TCGACAGTCAGCCG CATCTTCTTT-3′; GAPDH rev: 5′-ACCAAATCCGTTGACTCCGACCTT-3′.

Determination of viral vector copy number by real-time quantitative PCR

Genomic DNA from PLB-985 clonal populations was isolated using the DNeasy Blood & Tissue Kit (Qiagen GmbH, Hilden, Germany). Real-time quantitative PCR to determine VCN was performed using a Roche LightCycler 480 (Roche) applying advanced quantification (LightCycler 480 Software 1.5.0, Roche) with a reference sample known to harbor one single vector integrant in serial dilution (human XCGD PLB-985 clone) as described before.[42]

Western blotting

After differentiation transduced and sorted PLB-985 and control cells washed with ice cold PBS and subsequently lysed in 100 µl lysis buffer buffer (1% (v/v) Triton X-100, 150 mmol/l NaCl, 50 mmol/l Tris–HCl, Ph 7.4, 2 mmol/l EDTA). Protein concentrations were quantified by a standard Bradford assay. Equal amounts of protein per sample (30 µg) were run on 8% SDS polyacrylamide gels and electroblotted onto PVDF membranes that had been blocked using 4% milk powder in PBS-T. Membranes were incubated overnight at 4 °C with primary antibodies (mouse α-human gp91[phox] MoAB48, 1:500; rabbit α-actin, Santa Cruz), and peroxidase-conjugated secondary antibodies were used for detection (goat α-mouse/rabbit HRP, Santa Cruz, 1:5,000, 60 minutes, RT) in combination with the ECL detection kit Supersignal West Pico Chemiluminescent Substrate (Pierce, Rockford, IL).

Cytochrome C reduction assay

Differentiated cell populations were subjected to analysis as described before[21] using a Spectra MAX 340 reader (Molecular Devices, Sunnyvale, CA) and the SOFTmax Version 2.02 PRO software. The mean absorbance values of duplicates at 550 nm were converted based on the extinction coefficient of cytochrome c: $\Delta E_{550} = 21 \times 10^3$ mol/l^{-1} cm^{-1}. All chemicals were purchased from Sigma-Aldrich.

NBT assay

Granulocytes obtained after *in vitro* differentiation were sorted by FACS to obtain a pure population, of KD-vector expressing cells. Cells were subsequently pelleted and resuspended in prewarmed PBS supplemented with 1 mg/ml NBT and 2 µg/ml PMA (both Sigma-Aldrich). After 30 minutes at 37 °C cells were transferred on glass slides and photos were taken using a Nikon Eclipse TE300/DS-U1.

DHR assay

The DHR assays were performed as described previously.[43] Briefly, washed samples were subjected to surface marker staining in HBSS (Gibco) supplemented with 7.5 mmol/l D-Glucose, 0.5% BSA, 2,000 U/ml Catalase (C3155) and 5 µg/ml DHR123 at 37 °C. Following incubation at 37 °C for 10 minutes PMA was added to a final concentration of 0.1 µg/ml. Samples were further incubated for 15–20 minutes at 37 °C under agitation, the reaction was stopped on ice and the fluorescence signals were recorded using BD FACS Canto II, immediately. All chemicals were purchased from Sigma-Aldrich.

Animals and transplantation

NSG mice (NOD.Cg-*Prkdc*[scid]*Il2rg*[tm1Wjl]/SzJ) were obtained from Jackson Laboratories (Bar Harbor, ME). Animal experiments were approved by the regional council (Regierungspräsidium, Darmstadt, Germany) and conducted in compliance with the local animal experimentation guidelines. Two days post last transduction transduced human CD34+ cells were washed twice, resuspended in X-VIVO 10 medium (Lonza) and 10^6 cells were injected intravenously into sublethally irradiated (2.4 Gy) 8–9 week-old NSG mice. Mice were sacrificed 8 weeks later to isolate bone marrow that was then subjected to erythrocyte lysis (BD Pharm Lysis, BD Biosciences) and analysis (flow cytometry). Transplanted mice were kept in individually ventilated cages and drinking water was supplemented with 1.6 g/l neomycin for 2 weeks.

Statistical analysis

Statistical significance was calculated by unpaired or paired two-tailed t tests according to experimental design. Bar diagrams show mean + SD. *$P < 0.05$, **$P < 0.01$, ***$P < 0.001$.

CONFLICT OF INTEREST

The authors declare no conflict of interest.

shRNA-generated X-CGD cells for vector analysis
C Brendel et al.

12

ACKNOWLEDGMENTS

REFERENCES

1. Holland, SM (2013). Chronic granulomatous disease. *Hematol Oncol Clin North Am* **27**: 89–99, viii.
2. Roos, D (1994). The genetic basis of chronic granulomatous disease. *Immunol Rev* **138**: 121–157.
3. Segal, AW (1996). The NADPH oxidase and chronic granulomatous disease. *Mol Med Today* **2**: 129–135.
4. van den Berg, JM, van Koppen, E, Ahlin, A, Belohradsky, BH, Bernatowska, E, Corbeel, L *et al.* (2009). Chronic granulomatous disease: the European experience. *PLoS ONE* **4**: e5234.
5. Di Matteo, G, Giordani, L, Finocchi, A, Ventura, A, Chiriaco, M, Blancato, J *et al.*; IPINET (Italian Network for Primary Immunodeficiencies). (2009). Molecular characterization of a large cohort of patients with Chronic Granulomatous Disease and identification of novel CYBB mutations: an Italian multicenter study. *Mol Immunol* **46**: 1935–1941.
6. Cole, T, Pearce, MS, Cant, AJ, Cale, CM, Goldblatt, D and Gennery, AR (2013). Clinical outcome in children with chronic granulomatous disease managed conservatively or with hematopoietic stem cell transplantation. *J Allergy Clin Immunol* **132**: 1150–1155.
7. Güngör, T, Teira, P, Slatter, M, Stussi, G, Stepensky, P, Moshous, D *et al.*; Inborn Errors Working Party of the European Society for Blood and Marrow Transplantation. (2014). Reduced-intensity conditioning and HLA-matched haemopoietic stem-cell transplantation in patients with chronic granulomatous disease: a prospective multicentre study. *Lancet* **383**: 436–448.
8. Seger, RA (2010). Hematopoietic stem cell transplantation for chronic granulomatous disease. *Immunol Allergy Clin North Am* **30**: 195–208.
9. Kaufmann, KB, Büning, H, Galy, A, Schambach, A and Grez, M (2013). Gene therapy on the move. *EMBO Mol Med* **5**: 1642–1661.
10. Grez, M, Reichenbach, J, Schwäble, J, Seger, R, Dinauer, MC and Thrasher, AJ (2011). Gene therapy of chronic granulomatous disease: the engraftment dilemma. *Mol Ther* **19**: 28–35.
11. Zhen, L, King, AA, Xiao, Y, Chanock, SJ, Orkin, SH and Dinauer, MC (1993). Gene targeting of X chromosome-linked chronic granulomatous disease locus in a human myeloid leukemia cell line and rescue by expression of recombinant gp91phox. *Proc Natl Acad Sci USA* **90**: 9832–9836.
12. Kume, A and Dinauer, MC (1994). Retrovirus-mediated reconstitution of respiratory burst activity in X-linked chronic granulomatous disease cells. *Blood* **84**: 3311–3316.
13. Le Cabec, V, Calafat, J and Borregaard, N (1997). Sorting of the specific granule protein, NGAL, during granulocytic maturation of HL-60 cells. *Blood* **89**: 2113–2121.
14. Ott, MG, Schmidt, M, Schwarzwaelder, K, Stein, S, Siler, U, Koehl, U *et al.* (2006). Correction of X-linked chronic granulomatous disease by gene therapy, augmented by insertional activation of MDS1-EVI1, PRDM16 or SETBP1. *Nat Med* **12**: 401–409.
15. Stein, S, Ott, MG, Schultze-Strasser, S, Jauch, A, Burwinkel, B, Kinner, A *et al.* (2010). Genomic instability and myelodysplasia with monosomy 7 consequent to EVI1 activation after gene therapy for chronic granulomatous disease. *Nat Med* **16**: 198–204.
16. Björgvinsdóttir, H, Ding, C, Pech, N, Gifford, MA, Li, LL and Dinauer, MC (1997). Retroviral-mediated gene transfer of gp91phox into bone marrow cells rescues defect in host defense against Aspergillus fumigatus in murine X-linked chronic granulomatous disease. *Blood* **89**: 41–48.
17. Winkelstein, JA, Marino, MC, Johnston, RB Jr, Boyle, J, Curnutte, J, Gallin, JI *et al.* (2000). Chronic granulomatous disease. Report on a national registry of 368 patients. *Medicine (Baltimore)* **79**: 155–169.
18. Jones, LB, McGrogan, P, Flood, TJ, Gennery, AR, Morton, L, Thrasher, A *et al.* (2008). Special article: chronic granulomatous disease in the United Kingdom and Ireland: a comprehensive national patient-based registry. *Clin Exp Immunol* **152**: 211–218.
19. Nakamura, M, Murakami, M, Koga, T, Tanaka, Y and Minakami, S (1987). Monoclonal antibody 7D5 raised to cytochrome b558 of human neutrophils: immunocytochemical detection of the antigen in peripheral phagocytes of normal subjects, patients with chronic granulomatous disease, and their carrier mothers. *Blood* **69**: 1404–1408.
20. Moreno-Carranza, B, Gentsch, M, Stein, S, Schambach, A, Santilli, G, Rudolf, E *et al.* (2009). Transgene optimization significantly improves SIN vector titers, gp91phox expression and reconstitution of superoxide production in X-CGD cells. *Gene Ther* **16**: 111–118.
21. Mayo, LA and Curnutte, JT (1990). Kinetic microplase assay for superoxide production by neutrophils and other phagocytic cells. *Meth Enzymol* **186**: 567–575.
22. Mussolino, C, Morbitzer, R, Lütge, F, Dannemann, N, Lahaye, T and Cathomen, T (2011). A novel TALE nuclease scaffold enables high genome editing activity in combination with low toxicity. *Nucleic Acids Res* **39**: 9283–9293.
23. Santilli, G, Almarza, E, Brendel, C, Choi, U, Beilin, C, Blundell, MP *et al.* (2011). Biochemical correction of X-CGD by a novel chimeric promoter regulating high levels of transgene expression in myeloid cells. *Mol Ther* **19**: 122–132.
24. Zou, J, Sweeney, CL, Chou, BK, Choi, U, Pan, J, Wang, H *et al.* (2011). Oxidase-deficient neutrophils from X-linked chronic granulomatous disease iPS cells: functional correction by zinc finger nuclease-mediated safe harbor targeting. *Blood* **117**: 5561–5572.
25. Mukherjee, S, Santilli, G, Blundell, MP, Navarro, S, Bueren, JA and Thrasher, AJ (2011). Generation of functional neutrophils from a mouse model of X-linked chronic granulomatous disorder using induced pluripotent stem cells. *PLoS ONE* **6**: e17565.
26. Jiang, Y, Cowley, SA, Siler, U, Melguizo, D, Tilgner, K, Browne, C *et al.* (2012). Derivation and functional analysis of patient-specific induced pluripotent stem cells as an *in vitro* model of chronic granulomatous disease. *Stem Cells* **30**: 599–611.
27. Suzuki, N, Yamazaki, S, Yamaguchi, T, Okabe, M, Masaki, H, Takaki, S *et al.* (2013). Generation of engraftable hematopoietic stem cells from induced pluripotent stem cells by way of teratoma formation. *Mol Ther* **21**: 1424–1431.
28. Amabile, G, Welner, RS, Nombela-Arrieta, C, D'Alise, AM, Di Ruscio, A, Ebralidze, AK *et al.* (2013). *In vivo* generation of transplantable human hematopoietic cells from induced pluripotent stem cells. *Blood* **121**: 1255–1264.
29. Slukvin, II (2013). Hematopoietic specification from human pluripotent stem cells: current advances and challenges toward de novo generation of hematopoietic stem cells. *Blood* **122**: 4035–4046.
30. Chadwick, K, Wang, L, Li, L, Menendez, P, Murdoch, B, Rouleau, A *et al.* (2003). Cytokines and BMP-4 promote hematopoietic differentiation of human embryonic stem cells. *Blood* **102**: 906–915.
31. Kennedy, M, Awong, G, Sturgeon, CM, Ditadi, A, LaMotte-Mohs, R, Zúñiga-Pflücker, JC *et al.* (2012). T lymphocyte potential marks the emergence of definitive hematopoietic progenitors in human pluripotent stem cell differentiation cultures. *Cell Rep* **2**: 1722–1735.
32. Doulatov, S, Vo, LT, Chou, SS, Kim, PG, Arora, N, Li, H *et al.* (2013). Induction of multipotential hematopoietic progenitors from human pluripotent stem cells via respecification of lineage-restricted precursors. *Cell Stem Cell* **13**: 459–470.
33. Davidson, BL and McCray, PB Jr (2011). Current prospects for RNA interference-based therapies. *Nat Rev Genet* **12**: 329–340.
34. Tulpule, A, Lensch, MW, Miller, JD, Austin, K, D'Andrea, A, Schlaeger, TM *et al.* (2010). Knockdown of Fanconi anemia genes in human embryonic stem cells reveals early developmental defects in the hematopoietic lineage. *Blood* **115**: 3453–3462.
35. Cavazzana-Calvo, M, Fischer, A, Hacein-Bey-Abina, S and Aiuti, A (2012). Gene therapy for primary immunodeficiencies: Part 1. *Curr Opin Immunol* **24**: 580–584.
36. Aiuti, A, Bacchetta, R, Seger, R, Villa, A and Cavazzana-Calvo, M (2012). Gene therapy for primary immunodeficiencies: Part 2. *Curr Opin Immunol* **24**: 585–591.
37. Rivat, C, Santilli, G, Gaspar, HB and Thrasher, AJ (2012). Gene therapy for primary immunodeficiencies. *Hum Gene Ther* **23**: 668–675.
38. Gabriel, R, Lombardo, A, Arens, A, Miller, JC, Genovese, P, Kaeppel, C *et al.* (2011). An unbiased genome-wide analysis of zinc-finger nuclease specificity. *Nat Biotechnol* **29**: 816–823.
39. Gaj, T, Gersbach, CA and Barbas, CF 3rd (2013). ZFN, TALEN, and CRISPR/Cas-based methods for genome engineering. *Trends Biotechnol* **31**: 397–405.
40. Vafaizadeh, V, Klemmt, P, Brendel, C, Weber, K, Doebele, C, Britt, K *et al.* (2010). Mammary epithelial reconstitution with gene-modified stem cells assigns roles to Stat5 in luminal alveolar cell fate decisions, differentiation, involution, and mammary tumor formation. *Stem Cells* **28**: 928–938.
41. Zhang, CC, Kaba, M, Iizuka, S, Huynh, H and Lodish, HF (2008). Angiopoietin-like 5 and IGFBP2 stimulate ex vivo expansion of human cord blood hematopoietic stem cells as assayed by NOD/SCID transplantation. *Blood* **111**: 3415–3423.
42. Kaufmann, KB, Brendel, C, Suerth, JD, Mueller-Kuller, U, Chen-Wichmann, L, Schwäble, J *et al.* (2013). Alpharetroviral vector-mediated gene therapy for X-CGD: functional correction and lack of aberrant splicing. *Mol Ther* **21**: 648–661.
43. Brendel, C, Müller-Kuller, U, Schultze-Strasser, S, Stein, S, Chen-Wichmann, L, Krattenmacher, A *et al.* (2012). Physiological regulation of transgene expression by a lentiviral vector containing the A2UCOE linked to a myeloid promoter. *Gene Ther* **19**: 1018–1029.